EARTHQUAKE ENGINEERING AND STRUCTURAL DYNAMICS
Earthquake Engng Struct. Dyn. 2003; **32**:1773–1794 (DOI: 10.1002/eqe.301)

Considerations for the development of real-time dynamic testing using servo-hydraulic actuation

J. Zhao[1,*,†], C. French[1], C. Shield[1] and T. Posbergh[2]

[1]*Department of Civil Engineering, University of Minnesota – Minneapolis, 122 Civil Engineering Building, 500 Pillsbury Drive, SE, Minneapolis, MN 55455, U.S.A.*
[2]*Department of Electrical and Computer Engineering, University of Minnesota – Minneapolis, 4-174 Electrical Engineering and Computer Science Building, 200 Union St., SE, Minneapolis, MN 55455, U.S.A.*

SUMMARY

This paper presents a study of the use of servo-hydraulic systems in the implementation of real-time large-scale structural testing methods in force control such as effective force testing (EFT) and in displacement control such as real-time pseudodynamic testing (RPsD). Mathematical models for both types of control systems are presented and used to investigate the influences of servo-systems on the overall system performance. Parameters investigated include the overall system dynamics, nonlinearities of servo-systems, actuator damping, system mass including piston mass, and system response delay. Results of both numerical simulations and experiments showed that many of the influences of the servo-hydraulic system that significantly affect the real-time dynamic tests can be properly compensated through control schemes identified in this paper. Copyright © 2003 John Wiley & Sons, Ltd.

KEY WORDS: effective force testing; pseudodynamic testing; real-time dynamic testing; seismic simulation; hydraulic actuators; servovalve model

INTRODUCTION

Real-time dynamic testing is a powerful tool for the study of structural seismic response, especially when the test structure exhibits velocity dependent behaviors [1]. A shake table is often used to simulate the dynamic effects of earthquakes on structural models. However, structures tested on shake tables typically have to be scaled down due to limited table capacities. At smaller scales, it is difficult to investigate structural details such as anchorage of reinforcement in concrete and resistance mechanisms such as shear. In addition, tests with small-scale models may not accurately demonstrate the effect of structural control devices because of scaling.

* Correspondence to: J. Zhao, Department of Civil Engineering, University of Minnesota – Minneapolis, 122 Civil Engineering Building, 500 Pillsbury Drive, SE, Minneapolis, MN 55455, U.S.A.
† E-mail: zhao0058@umn.edu
Contract/grant sponsor: National Science Foundation (NSF); contract/grant number: CMS-9821076.

Received 6 March 2002
Revised 13 September 2002
Accepted 3 January 2003

Several alternatives to shake table testing have been studied to facilitate the investigation of the dynamic effects of earthquakes on large-scale structures. Among them are effective force testing (EFT) and real-time pseudodynamic testing (RPsD). Hydraulic actuators and a reaction floor/wall system are used to implement these test methods on structural systems that can be idealized with lumped masses [1–4]. A brief description of the methods is provided below.

In effective force testing, hydraulic actuators are used to apply **effective forces** (P_{eff}) to the center of each story mass of the test structure; these forces are the product of the story mass and the ground acceleration. Motions measured relative to the ground are equivalent to the response that a structure would develop relative to a moving base as in a shake table test or an earthquake event. Although the effective forces imposed in testing are independent of the structural stiffness and damping, a natural velocity feedback path (intrinsic to the servo-hydraulic system) combined with a force control algorithm required by EFT results in the inability of the actuators to apply effective forces near the natural frequency of the structure in the direct implementation of EFT. A velocity feedback correction with phase compensation can solve this problem and make the implementation of EFT successful [2, 3, 5].

For the pseudodynamic testing method, the equation of motion is solved incrementally to determine story displacements with respect to the ground for a given earthquake acceleration record. Hydraulic actuators are used to apply the **calculated relative displacements** to the structure. The restoring forces are measured at the individual story levels and used to calculate the next set of incremental story displacements. By using substructuring techniques, the structural lumped mass can be absent. This has an advantage in that less power may be required to achieve the required displacements. However, the lack of physical mass has a potential impact on the member behavior such as achieving a different stress state with reduced gravity loading.

Servo-systems can have a significant influence on these two testing systems. The performance of EFT can be affected by nonlinear flow properties of the servovalve (when large velocity responses are expected) [6], and the phase lag within servo-systems [3]. In addition, the actuator response delay may significantly aggravate the accuracy of RPsD, and even cause instability [4].

Although individual studies have provided some information regarding the effect of servo-systems on the test methods, it is of value to systematically investigate these influences to gain further insight. In this paper, the mathematical models of servo-hydraulic systems are first derived for computer simulations, and then simplified to facilitate linear system analysis. Both testing systems are analyzed to reveal the potential influences of servo-systems. Experimental validation is provided throughout the discussion of the parameters investigated.

For force-controlled test systems, the parameters investigated include overall system dynamics, the effect of actuator damping, nonlinearities and time delay in servo-systems, and effect of piston mass. For displacement-controlled test systems, the parameters are overall system dynamics, system response delay, system damping, system mass including the effect of piston mass, and nonlinearities in servo-systems.

MATHEMATICAL MODELS FOR DYNAMIC TESTING SYSTEMS

Component dynamics in the testing system

During a test involving servo-hydraulic actuation, a servovalve controller compares a command signal to a feedback signal and sends the generated valve command signal to the servovalve

to drive the valve spool. The spool controls the hydraulic fluid into the chambers of the actuator. The pressure difference between the two chambers multiplied by the actuator piston area produces the force applied to the test structure. In force-controlled tests the force measured by a load cell mounted on the actuator piston is fed back to the controller to close the control loop while in displacement-controlled tests the displacement measured by an LVDT is the feedback signal.

The valve command signal (v) can be expressed as

$$v = C_F[G_p(u - x) + G_d(\dot{u} - \dot{x})] \tag{1}$$

where u is the command signal, x is the feedback signal, $\dot{u}$ and $\dot{x}$ are the time derivatives of these signals, C_F converts these physical signals into voltage signals, and G_p and G_d are respectively the proportional and derivative gain settings in the servovalve controller, such as the MTS 407 used in this study.

The dynamics for a three-stage servovalve, such as the MTS 256.09 used in this study, can be described by the following equation

$$v = m_{ev}\ddot{x}_v + \beta_{ev}\dot{x}_v + k_{ev}x_v \tag{2}$$

where x_v is the main-stage spool opening ($-1 \leqslant x_v \leqslant 1$), and m_{ev}, β_{ev}, and k_{ev} are equivalent mass, damping, and stiffness of the servovalve, respectively. The product literature for the MTS 256.09 servovalve indicates that the second-order system is highly damped and its magnitude response rolls off at approximately 30 Hz.

The flow property of the servovalve, which relates the main-stage spool opening to the hydraulic flow it controls, can be formulated as

$$Q = K_v x_v \sqrt{1 - \frac{x_v}{|x_v|}\frac{p}{p_s}} \tag{3}$$

where Q is the flow into the actuator chambers, K_v is the main-stage servovalve flow gain, p_s is the hydraulic supply pressure, and p is the load pressure (the pressure drop across the piston) [7]. The nonlinearity introduced to the system through the square root term in Equation (3) is referred to as the **load pressure influence**.

The equation of conservation of mass is used to relate the hydraulic flow to the pressure difference (p) between the two chambers of the actuator [7]. Therefore the actuator dynamics are given by

$$Q = K_a\dot{p} + C_l p + A\dot{x} \tag{4}$$

where K_a is the hydraulic fluid compressibility coefficient, C_l is the leakage coefficient, A is the actuator piston area, and $\dot{x}$ is the piston velocity. Because the actuator and test structure are assumed rigidly connected, and the other end of the actuator is assumed attached to a rigid reaction wall, the movement of the actuator piston must equal the movement of the structural mass.

For simplicity, a SDOF system was used for the experimental investigation. Both viscous damping and Coulomb friction are considered in the following equation of motion:

$$pA - F_c = m\ddot{x} + c\dot{x} + kx \tag{5}$$

Table I. System parameters.

α	Constants in phase-lead networks	0.1
A	Actuator piston area	82.1 cm^2
c	Viscous damping of the structure	1.1, 2.1 kN-sec/m
c_m	Viscous damping in the modeled SDOF system (RPsD)	3.5 kN-sec/m
C_l	Leakage coefficient in actuator	0.1e − 8 m^5/kN/sec
C_F	Conversion factor (Force controlled)	0.056 V/kN
C_F	Conversion factor (Disp. controlled)	78.74 V/m
F_c	Coulomb friction in the structure	95.7 N, 31.6 N
G_p	Proportional gain in the analog controller	0.8059
G_d	Derivative gain in the analog controller	0.0
K_a	Coefficient related to fluid compressibility in actuator	0.3e − 8 m^5/kN/sec
K_s	Equivalent servovalve gain	0.1
K_v	Main-stage servovalve flow gain	1.6e − 2 m^3/sec
k	System stiffness	700.8 kN/m
m	Mass of the structure	7084 kg
m_m	Mass of the modeled SDOF system (RPsD)	7084 kg
p_s	Pressure supply	1.7e4 kN/m^2
T_d	Time constant of the phase-lead network (EFT)	5.0 ms
T_{ld}	Time constant of the amplitude compensation	68 ms
T_d	Time constant of the delay compensation	11.2 ms

where F_c is the Coulomb friction, and m, c, and k are respectively the test structure mass, damping, and stiffness. It should be noted that the mass and damping in Equation (5) are those physically present, and for the case of pseudodynamic testing, the physical mass and damping can be different from those mathematically modeled.

In summary, these equations describe the dynamics of a testing system under either force or displacement control. Although the performance of the testing system can be obtained by solving these differential equations simultaneously, computer simulations are usually used to obtain the system responses.

Computer simulation models

Computer simulations were conducted with SIMULINK® 3.0, a dynamic system simulation toolbox of MATLAB® version 5.3. Using the hydraulic models shown in Equations (1)–(4), the structural model in Equation (5), and the system parameters listed in Table I, computer simulation studies were conducted to verify the influences that the servo-system can have on the overall system.

A block diagram of the overall system for the force-controlled method is shown in Figure 1(a). A feedback path from the structural velocity response to the hydraulic flow into the actuator reflects the conservation of mass shown in Equation (4). The resulting loop is referred to as **natural velocity feedback**, which greatly limits the ability of the actuator to apply forces near the natural frequency of the structure [8]. An additional loop, **velocity feedback compensation** with phase adjustment (shaded blocks), is required for the successful implementation of EFT as demonstrated by Shield *et al.* [3].

Figure 1(b) illustrates the block diagram for a testing system under displacement control. The servo-system, the structure, and the interaction between them are the same as those

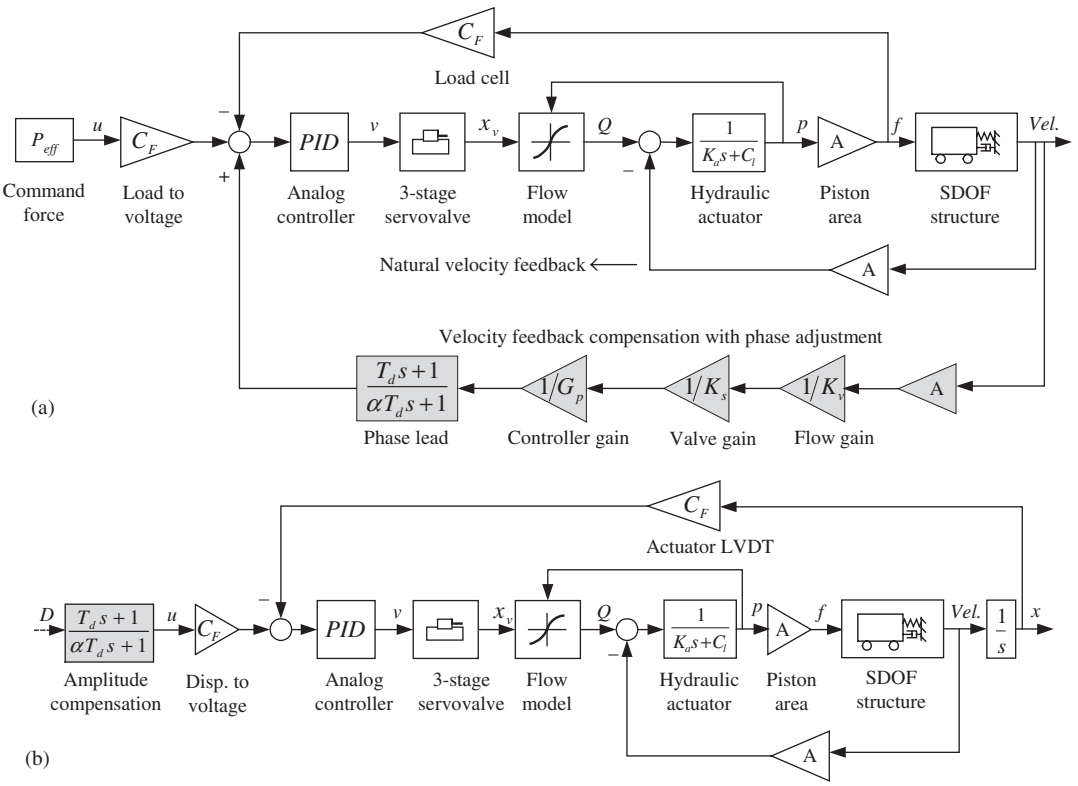

Figure 1. (a) Model of force-controlled testing system with linearized velocity feedback correction (shaded blocks). (b) Model of displacement-controlled testing system with amplitude compensation (shaded block).

of the force-controlled system while the hydraulic control is based on the actuator piston displacement instead of the actuator force. As will be demonstrated later in this paper, the amplitude compensation shown in the shaded block is necessary to achieve good position tracking performance.

To simplify the block diagram, masked blocks are used to represent the dynamics of the analog controller, the servovalve, and the SDOF structure. In addition to computer simulations using the nonlinear models, linear system analysis was used to provide closed form derivations and solutions for the linearized systems.

Models for linear system analysis

The dynamic systems modeled by high-order nonlinear differential equations can be approximated within a useful, though limited, range as linear systems. For low frequencies (below the roll-off frequency of the servovalve, i.e., 0–10 Hz in this study), the servovalve dynamics

shown in Equation (2) can be represented by the linear relation,

$$v = k_{ev} x_v \tag{6}$$

When the load pressure is small, the nonlinear flow model shown in Equation (4) can be simplified to the linearized approximation about the null position of the servovalve spool, such that the square root term is close to unity,

$$Q = K_v x_v \tag{7}$$

In addition, an equivalent viscous damping can be used to approximate the effect of the Coulomb friction (F_c) and the real viscous damping such that the equation of motion of the test structure becomes

$$pA = m\ddot{x} + c\dot{x} + kx \tag{8}$$

The linearized ordinary differential equations can be transformed into algebraic equations using operational mathematics, and techniques of control engineering such as root locus can be used to provide insight into the system behavior. The information obtained through computer simulation and linear analysis was validated in the laboratory using a nonlinear elastic SDOF structural model.

DESCRIPTION OF EXPERIMENTAL SETUP

The structural model consisted of a 7080 kg concrete mass atop four caster wheels with two springs on each side of the structure in the direction of motion as shown in Figure 2(a). The springs, which had a stiffness of 175.2 kN/m each, were precompressed to 2.5 cm prior to testing resulting in an initial system stiffness of 700.8 kN/m. The springs on either side of the mass were designed to lose contact with the mass at displacements exceeding 2.5 cm, resulting in a reduced stiffness of 350.4 kN/m. A measured force-displacement relation for the experimental setup is shown in an inset to Figure 2(a). An automobile suspension strut was used as a damper in some tests while a fluid viscous damper was used in others. The initial natural frequency of the system was 1.58 Hz.

To determine the system damping and the friction force without the actuator attached to the structure, a free vibration test with an initial displacement of 1.3 cm was conducted. Simulations based on Equation (5), with the excitation force (pA) set to zero, were made to determine the combination of viscous damping c and friction force F_c that minimized the error between the measured displacements and simulation results based on a least square technique. The resulting damping ratio and friction force were 0.8% of critical damping and 95.7 N, respectively. A comparison of the measured and simulated results is shown in Figure 2(b).

Forces or displacements were applied to the structure using a 170 kN hydraulic actuator equipped with a 5.7 l/sec three-stage servovalve. The additional control components, such as velocity feedback compensation for EFT, were implemented using a dSpace DS1102 DSP controller with a TI TMS320C31 floating-point digital signal processor with a 2 kHz sampling rate.

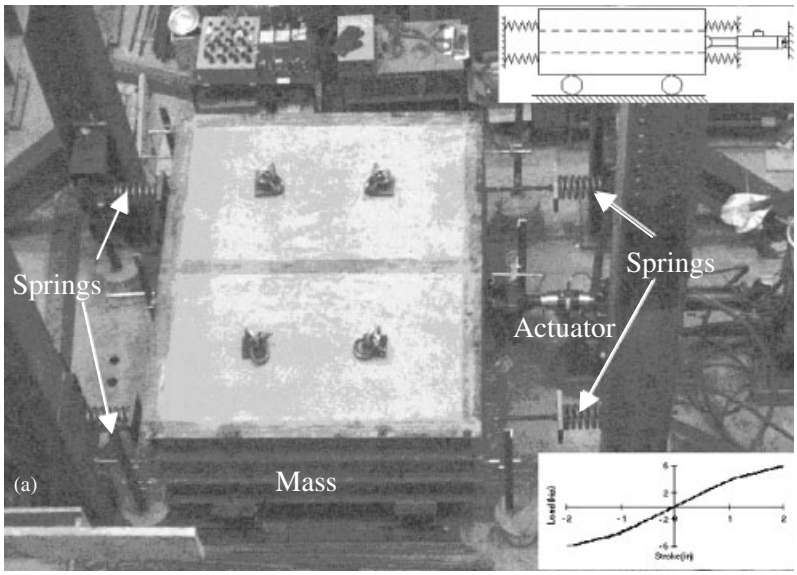

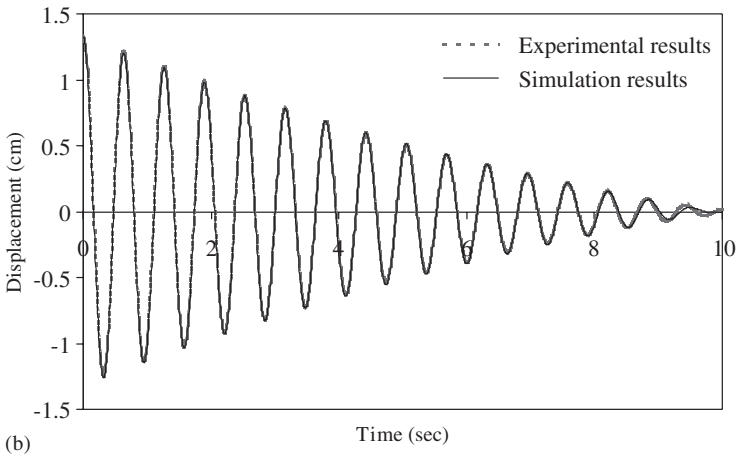

Figure 2. (a) The testing structure with the servo-hydraulic actuator. (b) Comparison of the simulation vs. free vibration test results.

TESTING SYSTEMS IN FORCE CONTROL

System dynamics

The transfer function (G_{fu}) for the linearized model for a testing system in force control, from the command force (u) to the applied force (f), is

$$G_{fu}(s) = \frac{AK_vC_FK_sG_p(ms^2 + cs + k)}{A^2s + (K_as + C_l)(ms^2 + cs + k) + AK_vC_FK_sG_p(ms^2 + cs + k)} \tag{9}$$

where, $K_s = 1/k_{ev}$, the valve gain. The numerator polynomial includes the denominator of the structure transfer function ($ms^2 + cs + k$); therefore, the poles of the structure are also zeros of the overall transfer function. This explains the significant amplitude reduction of applied forces near the natural frequency of the structure observed in the experimental study under a 2.3 kN sinesweep excitation (0–10 Hz) with direct implementation of EFT as shown in Figure 3(a).

With the velocity feedback compensation that incorporates the exact inverse of the forward dynamics, the transfer function becomes

$$G_{fu}(s) = \frac{AK_vC_FK_sG_p}{K_as + (C_l + AK_vC_FK_sG_p)} \tag{10}$$

The compensated system becomes a first-order system, for which the roll-off frequency is

$$\omega_{c\mathrm{EFT}} = \frac{C_l + AK_vC_FK_sG_p}{K_a} \tag{11}$$

The roll-off frequency for the system in this study was above 120 Hz, which was much higher than the frequency range of interest (0–10 Hz) and independent of the structural properties.

Figure 3(b) shows the performance of the compensated system under the same sinesweep excitation. As can be seen, the actuator was able to apply required forces over the entire excitation frequency range though a shallow drop can be identified over a range of frequencies (1 to 4 Hz). This was attributed to servo-system nonlinearities not accounted for in the linearized velocity feedback compensation scheme, which will be discussed in a later section on nonlinearity in servo-systems.

Hence the dynamics of the servo-system affect the direct implementation of EFT, especially when the effective forces have significant frequency content near the natural frequency of the structure. The methodology of velocity feedback compensation is able to negate such influences.

System damping

Another concern for force-controlled systems is the possibility that the actuator may add damping to the system. To determine the system viscous damping and Coulomb friction after the actuator is attached to the structure, several forced vibration tests were conducted, and simulations based on Equation (5) were made to fit the testing results. Measured forces were used as excitation input to the SDOF model and the same technique as used in the free vibration test was used to characterize the viscous damping and Coulomb friction. The average value of viscous damping was 1.5% of critical damping and Coulomb friction was 31.6 N for the system attached to the actuator.

Compared to the results obtained from the free vibration test, the attachment to the actuator slightly changed the energy dissipation of the testing system. The friction force decreased from 95.7 N to 31.6 N, which was due to a slight change in the direction of motion of the concrete mass. The viscous damping increased from 0.8% to 1.5% of critical damping, which was attributed to an additional source of energy dissipation (e.g., the movement of the actuator piston in the hydraulic fluid).

Equivalent viscous damping was generated through computer simulations to represent the combination of viscous damping and friction force such that similar responses could be obtained [9]. It was found that the system damping increased from 1.1% to 1.6% of critical

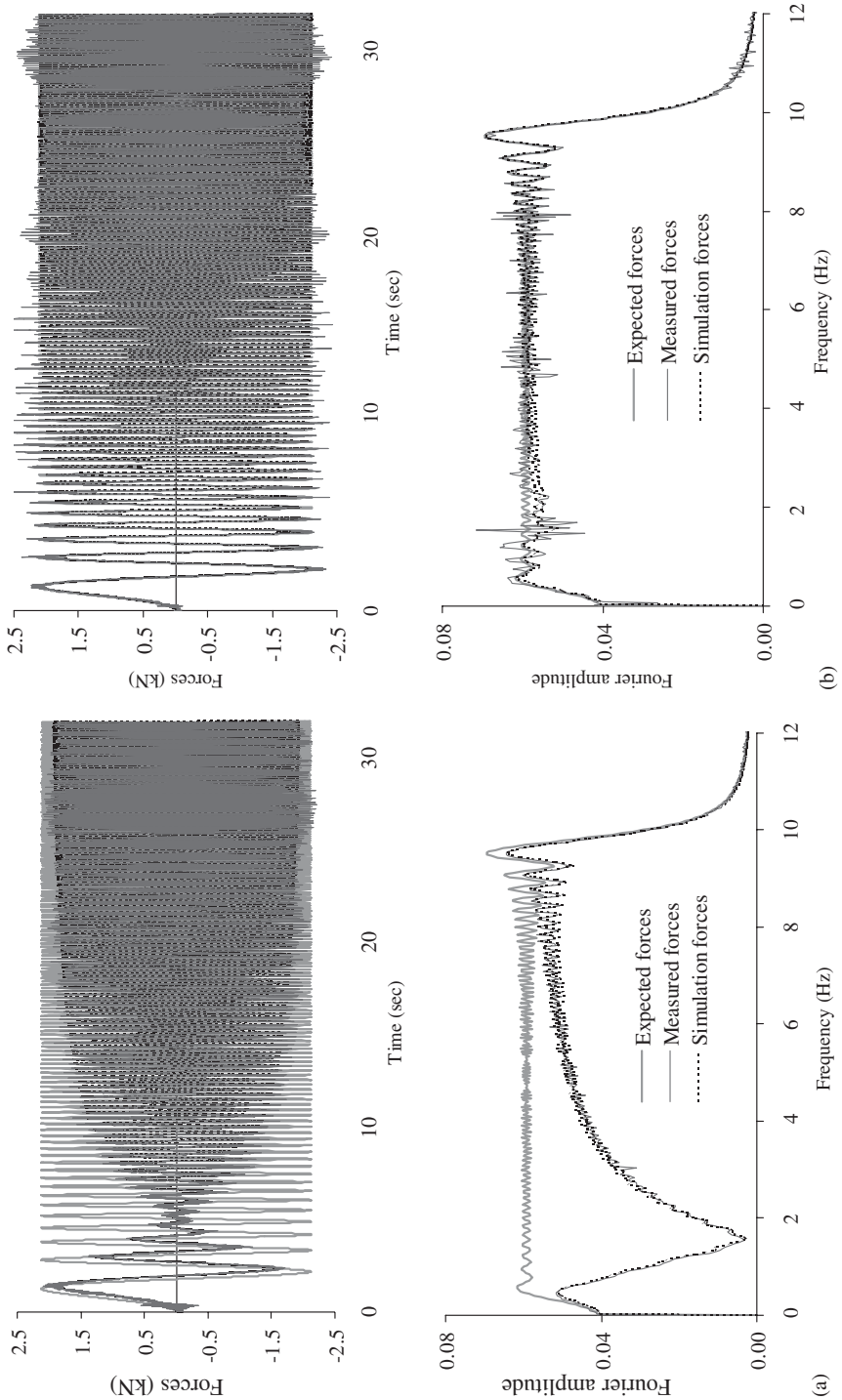

Figure 3. Comparison of expected vs. measured and simulation response for EFT. (a) Response without velocity feedback compensation. (b) Response with linear velocity feedback compensation.

damping after the actuator was attached. Because the energy dissipation through movement of the actuator piston was believed to be limited, the effect of the servo-system on overall system damping was deemed negligible.

Nonlinearity in servo-systems

As demonstrated in a previous section, simple linear compensation algorithms can generate good results as shown in Figure 3(b) for tests that require small spool opening (less than 10% for the servovalve in this study). However, significant nonlinearities exist in the servo-system and must be addressed for tests that require large spool openings. A constant initial flow gain was used in the linear system analysis and compensation, which was effective for small spool openings (less than 10%) as shown in Figure 4(a), which represents a typical flow-spool opening relationship. As can be seen, the flow gain K_v (i.e. the slope of the curve) decreases with an increase in spool opening. In addition, the load pressure influence as shown in Equation (3) is not negligible when the amplitude of the effective force is large compared with the load capacity of the actuator.

To investigate the potential influences of the servo-system nonlinearities on the system performance, a test was conducted using the linearized velocity feedback compensation scheme for the case of a large-amplitude excitation (8.9 kN) corresponding to a large spool-opening requirement. The Fourier amplitude of the measured forces shows a sharp drop in amplitude at the natural frequency of the test structure in Figure 4(b). Computer simulations were conducted for linear and nonlinear servovalve flow models in the forward path with the linearized velocity feedback compensation. The results from the simulation incorporating the nonlinear servo-system flow model explain the large amplitude drop.

The nonlinear flow-spool opening relation, such as the one shown in Figure 4(a), can be used in the feedback compensation to determine the corresponding compensation signal given the hydraulic flow to be compensated. A test incorporating the nonlinear relation in the compensation loop showed that the ability of the actuator to apply forces was greatly improved in Figure 4(c). A customized flow-spool opening relation and the load pressure influence should be incorporated in the compensation loop to remove the discrepancy adjacent to the natural frequency of the structure.

Because the velocity feedback compensation incorporates the inverse of the servo-system dynamics, accurate knowledge of the nonlinearities in servo-systems has been shown to be critical. The next section discusses the phase delay between compensation signals and command signals due to the response delay of the servo-system, which has been compensated in the tests shown in Figures 3 and 4.

Time delay in servo-systems

The influence of response delay of the servovalve on EFT was first noticed by Timm [5]. He noted that phase adjustment of the compensation signal was necessary before it was added to the command signal. However, only a portion of the response delay could be identified and the compensation was made through trial and error.

As shown in Figure 1(a), the piston area times the measured velocity of the structure or piston gives the flow to be compensated (also the flow affected by the natural velocity feedback loop). It is essential to ensure the same phase between the compensation flow and

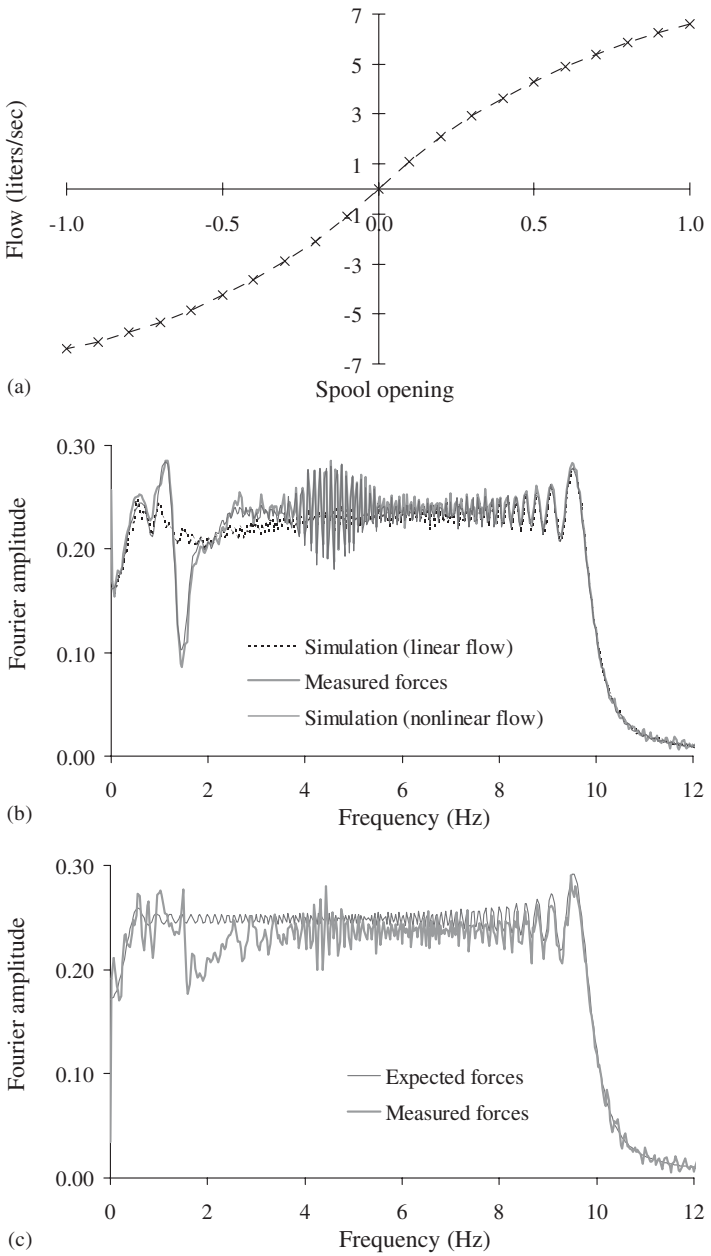

Figure 4. (a) A typical flow-spool opening relation. (b) Measured and simulation forces with linear velocity feedback compensation. (c) Measured forces with nonlinear velocity feedback compensation.

the flow caused by the natural velocity feedback. Because the compensation signal (addition to command signal) only goes through the servovalve and its controller before it meets the natural velocity feedback loop, any phase change caused by the dynamics of the servovalve and its controller must be removed. This also indicates that the delay to be compensated is independent of the test structure, and the compensation scheme can be used irrespective of the structural response.

Manufacturer product data indicated an **approximate** roll-off frequency of 30 Hz for the servovalve, the inverse of which was used to estimate the servovalve response delay (5.3 ms). Because the **exact** dynamics of the servovalve used was not known, a series of tests under small amplitude sinesweep excitations were conducted in conjunction with parametric simulations to finalize the time delay to be compensated (5 ms).

The phase-lead network shown in Figure 1(a) was used to make the phase adjustment to the compensation signal. Simulations indicated that if the phase compensation were not correct, a force amplitude peak would occur in the frequency domain at a smaller or larger frequency than the expected natural frequency corresponding to undercompensation or overcompensation of the response delay, respectively. Further analysis indicated that incorrect delay compensation could change the overall system dynamics, causing the dominant frequency of the structural response to drift from the natural frequency. In addition, overcompensation of the phase delay might lead to instability.

System mass

The system mass includes the mass of the actuator piston, which is usually not present in shake table tests and is not accounted for in analytical models. The piston in this study weighed approximately 54 kg, which represented less than 1% of the mass of the overall system. This would be expected in general for EFT because the actuator would typically be sized according to the structural mass and the peak ground acceleration [10]. Thus, the addition of piston mass to structural mass is negligible for the EFT method.

TESTING SYSTEMS IN DISPLACEMENT CONTROL

System dynamics

For testing systems in displacement control, a transfer function (G_{xu}) from the command position (u) to the displacement response (x) in the frequency domain can be derived as

$$G_{xu}(s) = \frac{AK_vC_FK_sG_P}{(C_l + K_as)(k + cs + ms^2) + A^2s + AK_vC_FK_sG_p} \tag{12}$$

The first term of the denominator is much smaller than the rest especially when the excitation frequency is around the natural frequency of the test structure. Thus the system can be approximated using a first-order transfer function. The equivalent roll-off frequency can be formulated as

$$\omega_{c\mathrm{RPD}} = \frac{K_vC_FK_sG_p}{A} \tag{13}$$

The frequency is 1.96Hz for the system with parameters listed in Table I. Figure 5(a) shows both the simulation and experimental results of such a system under a 1.27 cm sinesweep excitation. The amplitude of the measured and simulated displacement reduces as the excitation frequency increases. The reduction begins at zero frequency and reaches approximately 30% at 2 Hz. This indicates that amplitude compensation is necessary in order to obtain good position tracking performance.

Because the system dynamics was first-order dominant for low frequencies (less than 10 Hz), the amplitude reduction was compensated using the first-order phase-lead network shown in the shaded block of Figure 1(b). The time constant (T_d) was initially determined as the inverse of the roll-off frequency (81 ms). However, the proposed compensation scheme was affected by another component in the system, a slightly damped vibration mode due to the first term in the denominator that was neglected. The natural frequency of the vibration mode was estimated by

$$\omega = \sqrt{A^2/mK_a} \tag{14}$$

which is related to the so-called oil-column resonance.

As shown with dashed lines in Figure 6(a), the amplitude of the system response is slightly greater than that of the first-order approximation (gray lines) due to this additional vibration mode; therefore a smaller time constant should be used to achieve proper amplitude compensation. The position of the vibration mode in the frequency domain depends on the structural mass and the hydraulic fluid compressibility. If the physical mass were small, the vibration frequency would increase, thereby reducing its effect on the frequency range of interest.

The time constant can be determined through linear system analysis if the frequency range of the command signal to be compensated is known. A time constant of 68 ms was used in this study, the implementation of which resulted in a frequency response illustrated by a solid line in Figure 6(a). As can be seen, the acceptable performance was extended to a frequency of 5 Hz.

Responses of the compensated system to a 1.27 cm sinesweep displacement command are shown in Figure 5(b). The amplitude reduction was compensated with a slight overshoot. This was partly due to the amplitude amplification of the phase-lead network not being linear throughout the frequency range of operation. The excitation signal was stopped at 6 Hz because the required forces exceeded the actuator capacity when the actuator tried to track position signals with higher frequencies.

Equation (13) indicates that the system performance may be improved by tuning up the controller P-gain (G_p) such that the roll-off frequency is far from the frequency range of interest. However, there exists a limit of G_p for a given testing system because larger P-gain can cause instability. Following Routh's stability criterion [11], a relation between G_p and the system parameters can be formulated. Theoretically, G_p can be set large if the physically installed mass is very small (e.g. where only actuator piston mass is present). However, as indicated in Figure 6(b), the maximum P-gain decays exponentially with an increase of the physical mass. In practice, the physical mass, even when the substructuring technique is used, may be large enough to limit the P-gain setting such that the system performance is significantly affected.

In summary, the influence on the position-tracking ability of actuators due to overall system dynamics is shown in terms of two equivalent aspects: amplitude reduction and response delay. The influence can be compensated using a first-order phase-lead network because the

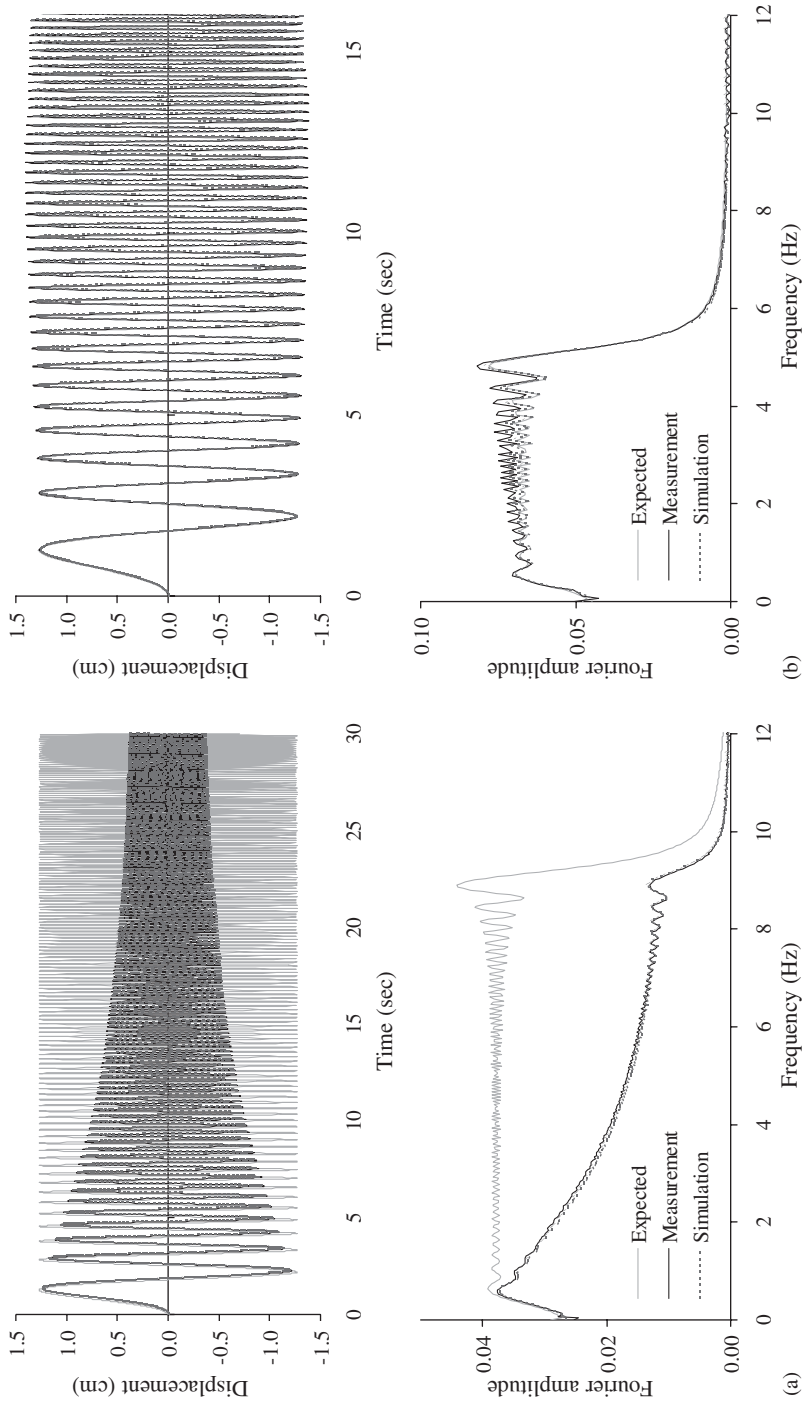

Figure 5. Comparison of expected vs. measured and simulation response for displacement-controlled tests. (a) Response without amplitude compensation. (b) Response with amplitude compensation.

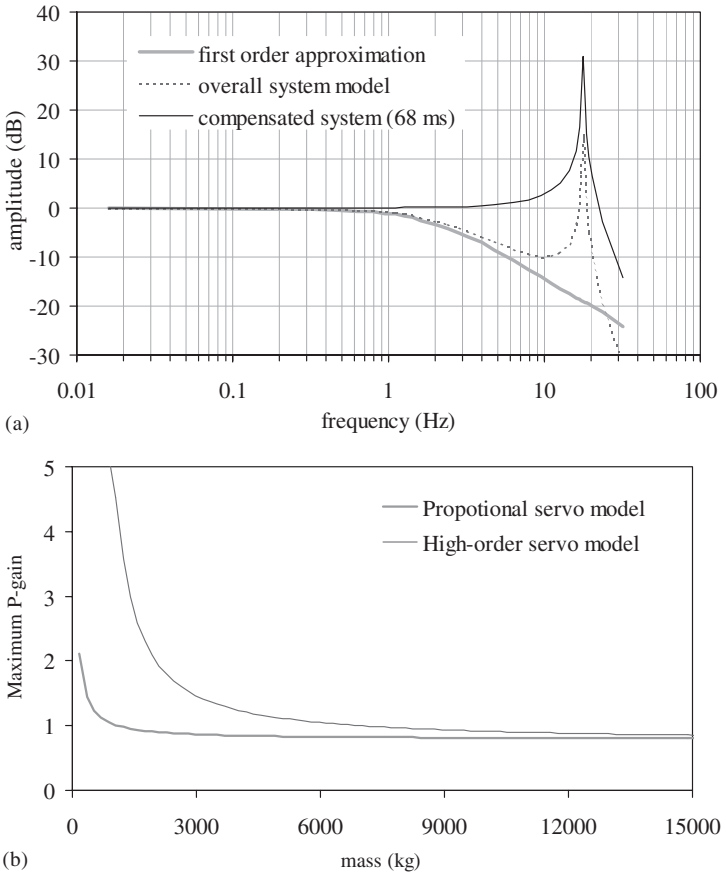

Figure 6. (a) The influence of the higher order dynamics to the amplitude compensation. (b) The relation between the maximum P-gain and the physical mass.

compensation scheme can amplify the amplitude as well as adjust the phase of the command signal. The physical mass can have an impact on the amplitude reduction and the performance of the compensation scheme.

Time delay of the system

The system response delay, estimated as the inverse of $\omega_{c\mathrm{RPD}}$ (81 ms in this study), has been partially negated by amplitude compensation. The remaining part of the response delay would affect tests such as RPsD because the on-line determination of the displacement command requires measured structural responses.

Horiuchi *et al.* [4] noted that the total system energy would increase if delayed responses were used to calculate restoring forces. However the concept was proved by computer simulations rather than experimental studies. Because the complex dynamics of the overall system were replaced by an electronic delay element, it was not able to reflect the influence of

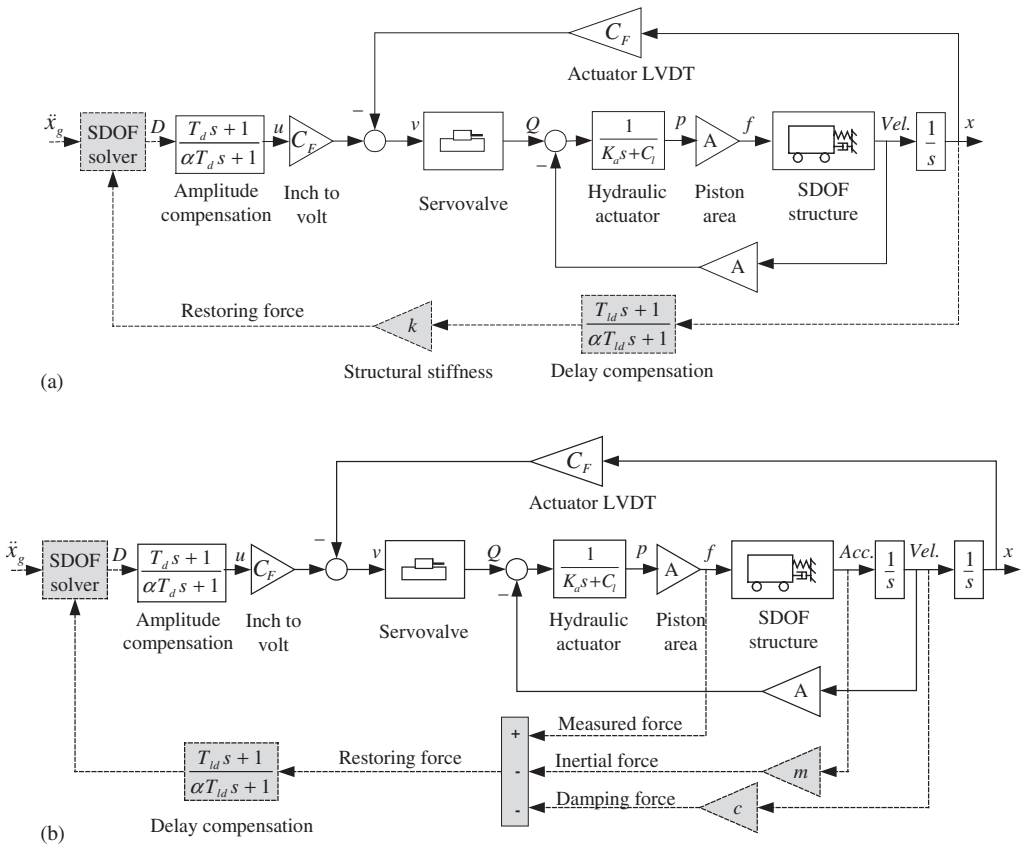

Figure 7. Model of the dynamic testing system in displacement control with on-line determined command signals. (a) Use measured displacement to determine the restoring force. (b) Use measured force to determine the restoring force.

the high-order system dynamics as described in this paper. The studies by Nakashima and Masaoka [1] showed that compensation for a portion of the total delay was made to obtain good amplitude match to command signals. The effect of the remaining part of the delay was not observed because the calculated displacement instead of the measured displacement was used to compute the restoring force.

The influence of the response delay on displacement-controlled testing systems was investigated experimentally using the testing system shown in Figure 7(a). The following equation of motion was solved incrementally using the central difference method and the explicit Newmark method discussed by Shing *et al.* [12, 13] to generate the command position signal (D):

$$m_m \ddot{x}_g = m_m \ddot{x} + c_m \dot{x} + f \tag{15}$$

where m_m and c_m are the modeled mass and damping, and f is the restoring force. The forces directly measured by the actuator load cell include inertial forces and damping forces in addition to restoring forces, which will be discussed in a later section. To simplify the

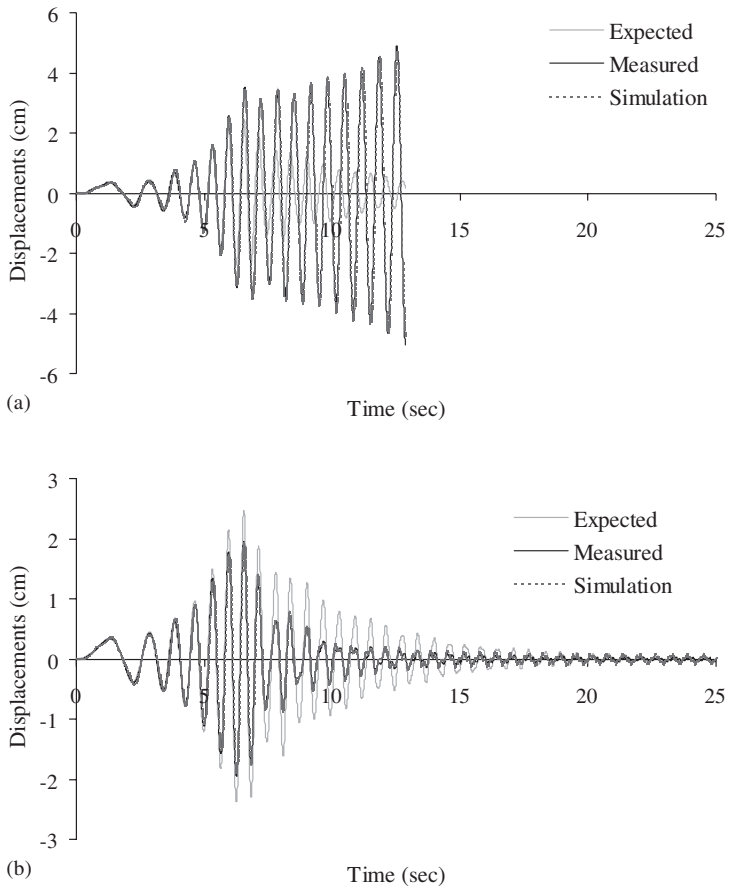

Figure 8. Comparison of the effect of the time-delay compensation. (a) Response with a time constant of 6 ms for delay compensation. (b) Response with a time constant of 16 ms for delay compensation.

determination of the restoring forces, the structure was kept in its linear range of behavior, and the measured displacement multiplied by the constant structural stiffness (k) was used.

A similar phase-lead network to the one used for the amplitude compensation was used to implement delay compensation for the generated restoring forces. The time constant T_{ld} in the response delay compensation was approximated as the difference between the **estimated** total response delay (81 ms) and the time constant of the amplitude compensation (68 ms). Because the **exact** system parameters and the influence of the additional vibration mode were not known, parametric simulations were conducted to finalize the time constant (11.2 ms) for this study.

Experimental tests with various delay compensation values (i.e. various values of T_{ld}) were conducted to investigate the effect of the response delay on the overall system; Sine wave sweeps (0–10 Hz, 0.15 g) were used as the ground acceleration input. The system response for the undercompensated case (i.e. 6 ms compensation) shown in Figure 8(a) indicated a

reduced system damping, which corroborated Horiuchi's hypothesis that using delayed response can introduce negative damping to the test system. In this test, the negative damping eventually caused the system response to become unstable. On the other hand, the test results for the overcompensated case (i.e. 16 ms compensation) shown in Figure 8(b) indicated that overcompensation for the response delay would increase the system damping and result in incorrect structural response.

In summary, unlike force-controlled systems, the response delay in displacement-controlled systems is caused by the overall system dynamics including the test structure though the contribution from the servo-system is dominant. Simple techniques such as the one used in this study are convenient and flexible in compensating for the response delay.

System damping

As discussed in the section on force-controlled test systems, the servo-system may add some damping to the testing system. In addition, the response delay compensation can affect the system damping as revealed in the previous section. Other influences on the system damping of displacement-controlled testing systems, such as the solver and means to determine the restoring forces, are investigated in this section.

Free vibration tests were designed, in which the structure was slowly pulled away from its neutral position by the actuator until the displacement reached 1.6 cm. The position command was obtained by solving the equation of motion shown in Equation (13) on-line with a ramp force input. Then the force input to the solver was set to zero, and the structure was released. Tests were conducted for cases when either calculated or measured displacements were used to calculate the restoring forces.

When calculated displacements were used to determine the restoring forces, the test system could be represented by Figure 1(b) with a solver in front of the amplitude compensation block. As shown in Figure 9(a), the measured structural response follows the expected response closely; indicating that the servo-system does not affect the structural response as long as proper amplitude compensation (68 ms) is employed. Computer simulation was able to predict the behavior of the test system. The delay compensation (11.2ms) was not applied because the calculated response had no phase difference with respect to the displacement command.

When measured displacements were used to calculate the restoring forces as shown in Figure 7(a), another closed loop formed in the system. The additional loop changed the overall system dynamics including the system damping. Results of the test are shown in Figure 9(b), which incorporate both the amplitude compensation (68 ms) and the response delay compensation (11.2 ms). The structural response shows a slightly different damping because the measured response does not follow the expected response exactly.

The additional loop includes the solver, which means that errors in system response and data acquisition can accumulate during a test. The response amplitude remains constant after 10 seconds rather than damping out as shown in Figure 9(b). Computer simulations were conducted that determined this behavior could result from a restoring force error of $0.03\sin(\omega_n t - \pi/2)$ kN. Although the nature of the error is currently not clear, possible sources are overshooting caused by the amplitude compensation, as well as the change of the overall system dynamics after the additional loop is closed.

In summary, the system damping is affected by the measured responses (i.e., displacements or forces) when measured responses are used to determine the restoring forces required in the

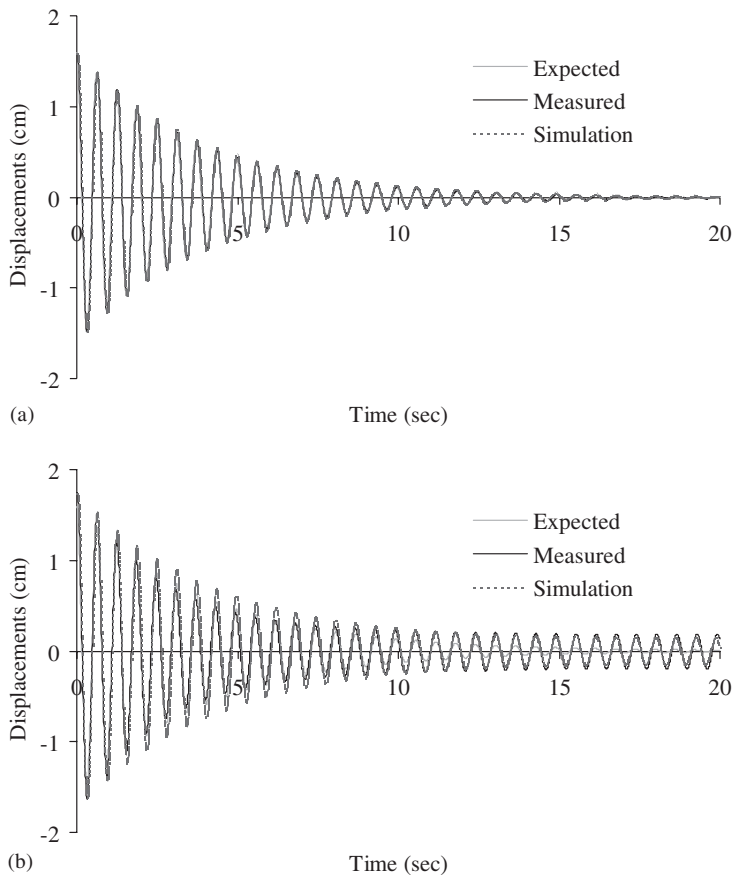

Figure 9. Free vibration in displacement control. (a) Use calculated displacements to determine restoring forces. (b) Use measured displacements to determine restoring forces.

solver. The next section discusses some problems one can have when using force measurements directly as the restoring forces.

System mass

When the test is conducted in real time, the actuator load cell will capture the damping and inertial force in addition to the restoring force. As can be seen in a test shown in Figure 10(a), where calculated displacements were used to determine the restoring forces, the load cell reading (pA) was vastly different from the required restoring force (f), which is the product of the measured displacement and the structural stiffness (kx) in this study. Theoretically the measured force should be the force input to the SDOF solver as indicated by the simulation shown in Figure 10(a).

One way to eliminate the effect of the inertial term and the damping term is to subtract these two terms from the force measurement as shown in Figure 7(b). This technique requires two more measurements: structural acceleration and velocity. It should be noted that additional

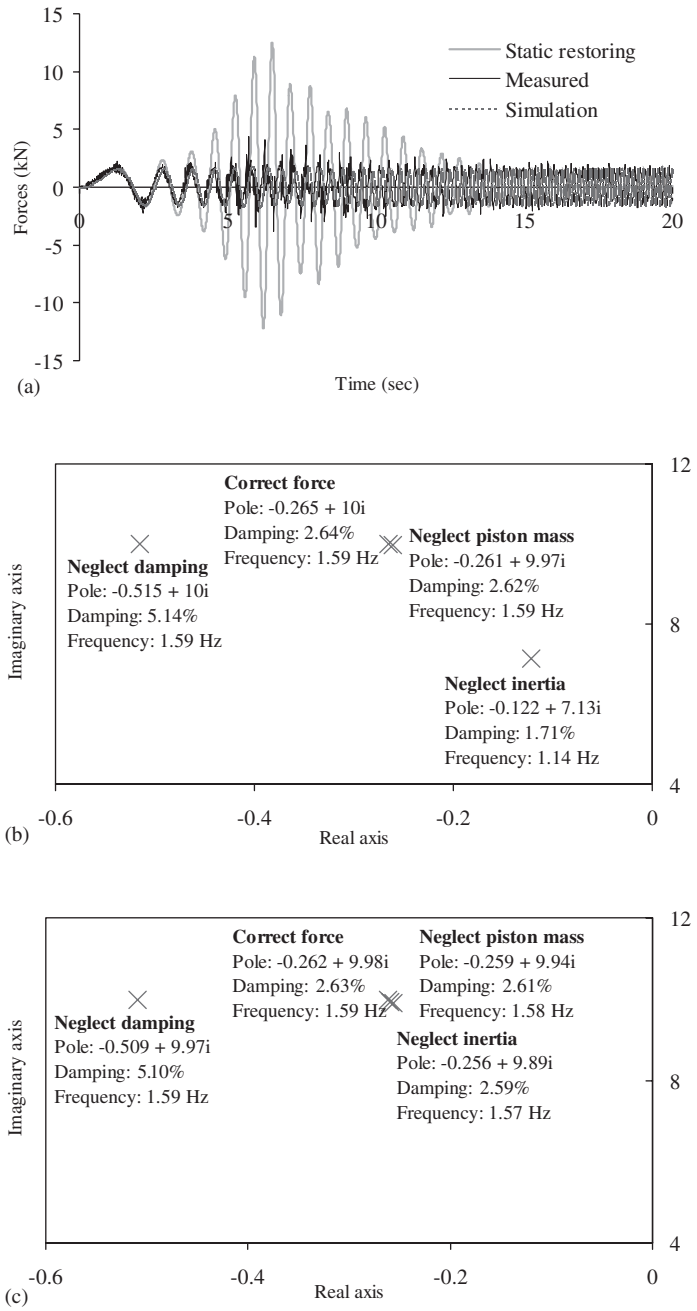

Figure 10. (a) Comparison of the measured forces vs. restoring forces. (b) Effect of incorrect restoring force (physical mass = modeled mass). (c) Effect of incorrect restoring force (physical mass = 2% of modeled mass).

loops formed here would affect the system damping in a similar way as discussed in the previous section.

Figure 10(b) shows the impact on the system performance in terms of a pole-zero map when the damping and inertial terms are not subtracted from the force measurement. The linear analysis of such a system indicates that using the force measurement directly in the solver changes the structural response dramatically, while keeping the damping term in the restoring force causes incorrect system damping. Although the piston mass (54 kg) is negligible compared to the structural mass (7080 kg), ignoring its contribution to the inertial term slightly changes the dominant frequency of the structural response.

The effect of the inertial force can be reduced when the substructuring technique is applied and the installed mass is small. If the physically installed mass is 2% of the modeled mass (140 kg), while the stiffness and damping remain the same, Figure 10(c) shows a linear system analysis of the new system in terms of a pole-zero map. In this case, similar observations can be made though the effect of ignoring the contribution of the inertial term in the restoring force is greatly reduced.

Nonlinearity in servo-systems

Although the proposed compensation algorithms are simple and can provide good performance as shown in Figure 5(b), significant nonlinearities such as the nonlinear servovalve flow property and load pressure influence can affect the implementation of these compensation schemes. As the required spool opening increases, the flow gain K_v reduces, indicating reduced performance of the servo-system. Thus the time constants of the proposed compensation schemes determined using the linearized system model and the initial flow gain may not be adequate throughout the operating range of the servo-system. The load pressure also affects the servo-system performance by limiting the hydraulic flow into the actuator.

These nonlinearities were observed in some tests that required large spool opening. For example, in the test shown in Figure 8(a), the maximum spool opening reached 28%. Both nonlinear flow properties of the servovalve and load pressure influence were needed in the computer simulation to match the measured results.

These results indicate that the nonlinearities of servo-systems can have significant impact on the implementation of displacement-controlled testing systems, and more advanced compensation schemes are necessary for these cases.

CONCLUSIONS

Effective force testing and real-time pseudodynamic testing are two testing methods under development for large-scale structures. Servo-hydraulic actuation is typically involved in the implementation of both methods. As a key component, servo-systems can have a significant influence on the performance of the two testing methods. Compensation schemes are necessary for the successful implementation of the two testing methods.

The velocity feedback compensation required by EFT relies on an accurate model of the forward dynamics of the test system such as the servovalve flow property. Although considering nonlinearities and response delay of servo-systems in the velocity feedback compensation are necessary, the implementation of the compensation scheme is independent of the test

structure. In addition, the piston mass and actuator damping have insignificant effects on the EFT method.

For displacement-controlled systems, overall system dynamics cause the amplitude reduction and response delay. The physically installed mass affects the level of the amplitude reduction (or the total response delay) by limiting the maximum P-gain setting. Simple first-order phase-lead networks can be used to compensate the system if hydraulic demands are small during the test. Otherwise, more advanced compensation schemes are necessary to account for nonlinearities in servo-systems.

The response delay needs to be compensated if the measured response is used in determining the command signal for the next step, otherwise, the system damping can be greatly affected. Forces measured by an actuator load cell include inertial and damping terms in addition to restoring forces. Use of the direct force measurements could significantly affect the structural response, which is represented by the change of the natural frequency and damping of the test structure.

In spite of the significant influences of servo-systems on real-time dynamic testing methods, results of simulation and experimental studies indicate that satisfactory response can be obtained using both testing methods, as long as appropriate compensation schemes identified herein are employed.

ACKNOWLEDGEMENT

Funding for this project was provided by the National Science Foundation (NSF) under grant number: CMS-9821076. Information contained herein does not necessarily represent the views of the sponsor.

REFERENCES

1. Nakashima M, Masaoka N. Real-time on-line test for MDOF systems. *Earthquake Engineering and Structural Dynamics* 1999; **28**:393–420.
2. Dimig J, Shield C, French C, Bailey F, Clark A. Effective force testing: a method of seismic simulation for structural testing. *Journal of Structural Engineering* (ASCE) 1999; **125**:1028–1037.
3. Shield C, French C, Timm J. Development and implementation of the effective force testing method for seismic simulation of large-scale structures. *Philosophical Transaction of the Royal Society* (*Theme Issue on Dynamic Testing of Structures*) 2001; **A 359**:1911–1929.
4. Horiuchi T, Inoue M, Konno T, Namita Y. Real-time hybrid experimental system with actuator delay compensation and its application to a piping system with energy absorber. *Earthquake Engineering and Structural Dynamics* 1999; **28**:1121–1141.
5. Timm J. *Natural velocity feedback correction for effective force testing*. Master's thesis 1999; Civil Engineering, University of Minnesota, Minneapolis. U.S.A.
6. Zhao J, French C, Shield C, Posbergh T. Development of EFT for nonlinear SDOF systems. *Proceedings of the 7th National Conference on Earthquake Engineering*, Boston, MA, 2002.
7. Merritt EA. *Hydraulic Control System*. Wiley: New York, 1967.
8. Dyke SJ, Spencer BF, Quast P, Sain MK. Role of control-structure interaction in protective system design. *Journal of Engineering Mechanics* (ASCE) 1995; **121**:322–338.
9. Chopra AK. *Dynamics of Structures: Theory and Applications to Earthquake Engineering*. Prentice-Hall: Englewood Cliffs, NJ, 1995.
10. Spink MJ, *MDOF implementation of effective force testing: a method of seismic simulation.* Master's thesis 2002; Civil Engineering, University of Minnesota, Minneapolis, U.S.A.
11. Franklin GF, Powell JD, Emami-Naeini A. *Feedback Control of Dynamic Systems* (3rd edition). Addison-Wesley: Boston, MA, 1994.
12. Shing PB, Nakashima M, Bursi OS. Application of pseudodynamic test method to structural research. *Earthquake Spectra* 1996; **12**:29–56.
13. Shing PB, Mahin SA. Experimental error effects in pseudodynamic testing. *Journal of Engineering Mechanics* (ASCE) 1990; **116**:805–821.

